The Boron Hardenability Effect in Thermomechanically Processed, Direct-Quenched 0.2 Pct C Steels

K.A. TAYLOR and S.S. HANSEN

The segregation and precipitation of boron have been studied in thermomechanically processed 0.2C-0.6Mn-0.5Mo steels containing nominally 0, 10, 20, 50, and 100 ppm B. These steels were hot-rolled in the laboratory (in simulation of production multipass rolling), and their transformation behavior during subsequent water quenching was examined for different finish-rolling temperatures (980 °C and 870 °C) and quenching temperatures (730 °C to 950 °C). The results showed that in general, a "free" boron content of 10 to 20 ppm (which is similar to the levels used for conventional quenched-and-tempered steels) will provide a boron hardenability increment similar to that for conventional quenched-and-tempered steels. The delay time prior to quenching (over the range of 10 to 100 seconds) did not have a significant effect on hardenability except in the steels containing 50 or more ppm B. In these higher B steels, precipitation of borocarbides occurred along austenite grain boundaries with a resultant decrease in hardenability.

I. INTRODUCTION

BORON is often used for economically increasing the hardenability of steels. When present at low levels (5 to 30 ppm B is typically used in conventionally quenched-and-tempered steels) and adequately protected from nitrogen, *i.e.*, from forming boron nitride, boron can typically increase the hardenability of low-alloy steels by a factor of 2 to 3.[1] The behavior of boron in austenitized-and-quenched (herein referred to as "reheat-quenched") steels has been studied extensively,[2] and it is clear that boron segregates to the austenite grain boundaries and increases hardenability by suppressing the nucleation of ferrite.

The steel industry has devoted considerable effort toward combining processing steps as a means of reducing costs and increasing overall efficiency. For example, some producers have eliminated a heat-treatment step for rolled products (heat-treated plates and rails) by installing in-line water-quenching units, thereby permitting the quenching of these products immediately after hot working (herein referred to as "direct quenching"). From a metallurgical point of view, the capability of combining hot working with water quenching raises a host of issues, including whether or not boron-treated martensitic or bainitic steels can be processed reliably in such units. In contrast to a conventional off-line isothermal austenitizing treatment (reheat quenching), the austenite cools continuously and generally undergoes repeated deformation and recrystallization during hot working prior to direct quenching. Since the segregation of the boron to the austenite grain boundaries requires diffusion and is thus time-dependent, there is some question as to whether the boron hardenability effect will always be operative in a thermomechanically processed steel.

Recent investigations of thermomechanically processed low-carbon steels containing about 10 ppm B[3,4] found that after high-temperature deformation and rapid subsequent recrystallization of the austenite, the boron segregated to the austenite grain boundaries very rapidly and a "normal" boron hardenability increment was obtained. However, when the deformation temperature was lowered so that recrystallization did not occur, the hardenability was generally found to be lower. This was attributed either to a lack of sufficient boron to neutralize the ferrite nucleation sites within the deformation substructure or, in some cases, to strain-induced precipitation of borocarbides (which presumably deplete the austenite grain boundaries of elemental boron).

The present investigation was undertaken to further define the behavior of boron in thermomechanically processed steels. Considering that the notch toughness of direct-quenched martensitic steels can generally be improved by conducting deformation below the austenite recrystallization temperature,[5,6,7] we specifically sought to define the range of boron content over which maximum hardenability could be obtained in steels containing unrecrystallized austenite after rolling. A series of 0.2C-0.6Mn-0.5Mo steels with nominal boron contents between 0 and 100 ppm was examined in this work and processed in the laboratory to simulate the commercial hot rolling of steel plates. This processing included deformation schedules that resulted in fully equiaxed as well as severely deformed austenitic grain structures prior to quenching. A laboratory hardenability test for as-rolled plate samples[8] was used in this work to obtain quantitative hardenability data, and the distribution of boron in these steels was determined qualitatively by optical and electron microscopy and by boron autoradiography.

II. MATERIALS AND PROCEDURES

A. *Preparation of Heats*

Five experimental 0.2C-0.6Mn-0.5Mo-B steels with nominal boron levels between 0 and 100 ppm were prepared as vacuum induction-melted, 227-kg ingots with a cross section of 200 by 200 mm; compositions for these steels are provided in Table I. Each heat was deoxidized with aluminum, then titanium was added to "stabilize" nitrogen (which otherwise might react with boron to form

K.A. TAYLOR, Research Engineer, and S.S. HANSEN, Supervisor, are with the Research Department, Bethlehem Steel Corporation, Bethlehem, PA 18016.

Manuscript submitted August 9, 1989.

Table I. Compositions (Weight Percent) of the Experimental Steels

Steel	C	Mn	P	S	Si	Ni	Cr	Mo	Ti	Al	B (ppm)	N (ppm)	Ti:N
0 B	0.18	0.60	0.006	0.005	0.25	0.016	<0.01	0.53	0.033	0.034	2	91	3.6
10 ppm B	0.19	0.61	0.006	0.004	0.26	0.016	<0.01	0.53	0.032	0.034	10	99	3.2
20 ppm B	0.18	0.63	0.006	0.005	0.24	0.016	0.028	0.52	0.033	0.032	19	73	4.5
50 ppm B	0.20	0.58	0.006	0.004	0.24	0.013	<0.01	0.52	0.033	0.034	49	97	3.4
100 ppm B	0.20	0.58	0.006	0.004	0.24	0.013	<0.01	0.53	0.034	0.042	96	83	4.1

boron nitride) as titanium nitride (TiN), and finally boron was added in the form of ferroboron. While the titanium additions to the present steels were based on a simple TiN stoichiometric approach (a Ti:N ratio of at least 3.4 was sought), the experimental results of Kapadia *et al.*[9] are consistent with this approach for nitrogen levels in the 50 to 100 ppm range (*i.e.*, similar to the nitrogen contents of the present steels). With the exception of the 10 ppm B steel, each of the B-containing steels contained adequate Ti to combine with all of the N. The Ti:N ratio of 3.2 for the 10 ppm B steel indicates that it contained a small amount of "free" nitrogen (about 5 ppm).

Each ingot was subsequently hot-rolled to a 100-mm-thick by 125-mm-wide slab. Billets 150-mm long were cut from the slabs. Midthickness holes were drilled to accommodate thermocouples for monitoring temperature during the subsequent rolling of the billets.

B. *Hardenability Tests*

The as-rolled hardenability of the experimental steels was measured with plate samples quenched directly off a laboratory rolling mill. This hardenability test entails immersing one end of the as-rolled plate into a tank of still water (Figure 1)[8] and is analogous to the Jominy test for reheat-quenched steels. Billets for these "end-quenching" tests were reheated to 1260 °C and rolled in 12 passes (to simulate production hot rolling) to a thickness of 19 mm (with a width of 125 mm and length of 610 mm), finishing at either 980 °C or 870 °C. These two rolling schedules are illustrated schematically in Figure 2, and the aim thickness and temperature for each rolling pass are given in Table II.

After the final rolling pass, each plate was held for a specified period of time (which varied between nominally 10 and 150 seconds) prior to quenching. Each plate was allowed to air cool during this delay interval; hence, the actual quenching temperature was sometimes significantly below the finish-rolling temperature. Following this delay, approximately one-half to two-thirds of the total length of each plate was immersed in a tank containing 58 L of still water at 12 °C to 18 °C. Each plate was kept in the quenching tank for 15 minutes and then was air-cooled. (The results obtained from these air-cooled samples were not significantly different from results obtained in tests in which the tank was completely filled with water after the 15-minute hold to fully quench the plate.) Figure 3 shows the actual variation in cooling rate

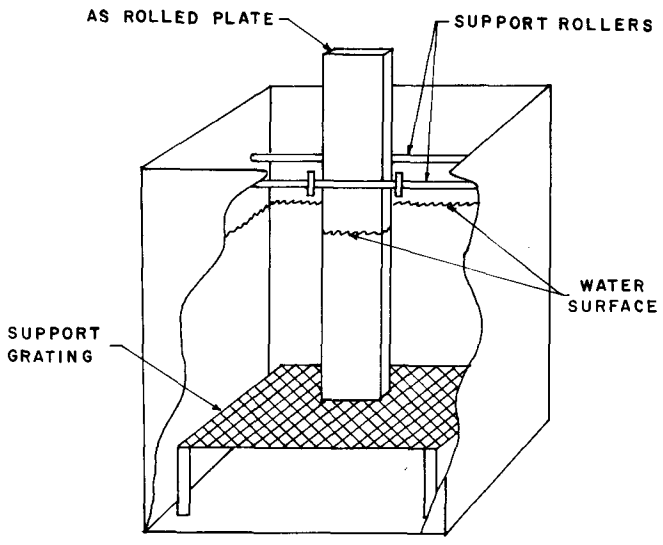

Fig. 1—Apparatus for end-quenching experiments.

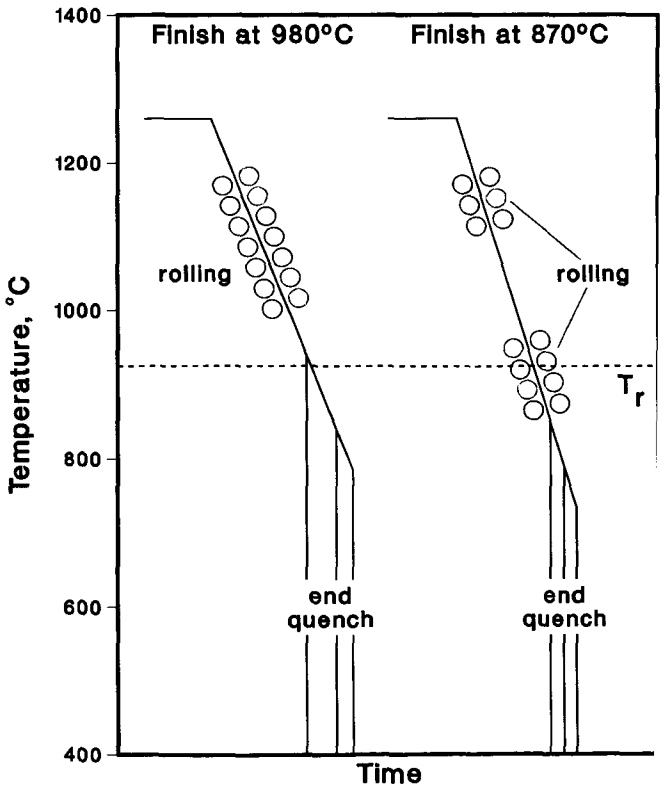

Fig. 2—Schematic temperature-time histories for plates used in end-quenching experiments. T_r denotes a temperature below which recrystallization of the austenite does not occur.

Table II. Rolling Schedules for the End-Quench Hardenability Tests

Pass	Thickness after Pass (mm)	Aim Temperature (°C) Finishing at 980 °C	Finishing at 870 °C
0	101.6	reheat (1260)	
1	99.1	1166	
2	88.9	1152	
3	76.2	1138	
4	63.5	1124	
5	53.3	1110	999
6	47.0	1093	982
7	40.6	1077	966
8	35.6	1060	949
9	30.5	1043	932
10	25.4	1027	916
11	21.6	1004	893
12	19.1	982	871

(averaged between 815 °C and 480 °C) measured at the center of an end-quenched 19-mm-thick plate as a function of distance from the water surface.[8] The cooling rate varied between about 31 °C/s at 75 mm below the surface of the water to about 1 °C/s at 75 mm above the surface of the water. This maximum cooling rate is approximately equivalent to the cooling rate encountered 8.4 mm from the quenched end of a standard Jominy bar.[10]

The important parameters for each end-quenching experiment are summarized in Table III, which lists the actual finishing temperatures, delay times, and quenching temperatures. This table shows that as the delay is increased from 10 to 100 seconds, the quenching temperature drops from about 940 °C to about 790 °C for plates finished at 980 °C and from about 850 °C to about 740 °C for plates finished at 870 °C.

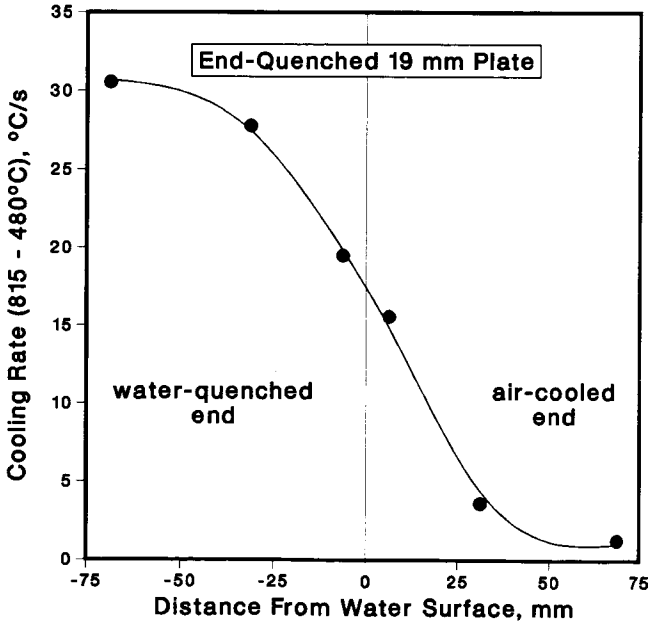

Fig. 3—Cooling rate (averaged between 815 °C and 480 °C) at the center of an end-quenched, 19-mm-thick (by 125-mm-wide) plate as a function of distance from the water surface.

Following quenching, specimens 150 mm in length and about 30 mm in width were removed from each plate, as indicated in Figure 4. The longitudinal faces perpendicular to the rolling plane were surface-ground, and hardness measurements (Rockwell C scale—HRC) were performed along the plate centerline on the face corresponding to the plate midwidth (Figure 4). Ideal critical diameters (D_I), representing the largest round section within which a microstructure containing at least 50 pct martensite can be formed throughout, were determined from these hardness profiles by

(1) noting the position on a given hardenability specimen at which the 50 pct martensite hardness was attained,
(2) estimating the cooling rate at that point (from Figure 3),
(3) determining the equivalent position on a standard Jominy bar (from Figure 5), and
(4) estimating the equivalent diameter of an ideally quenched, round bar from the known correlation between Jominy position and D_I[11] (from Figure 6).

The 50 pct martensite hardness for the present steels containing 0.18 to 0.20 pct C was taken to be 31 HRC, based upon a previously established relationship between 50 pct martensite hardness and carbon content.[12]

C. *Optical and Electron Microscopy*

Full-thickness specimens for optical microscopy were removed from end-quenched plates at locations which had been about 75 mm below the water surface and thus had been cooled at the maximum achievable rate (about 31 °C/s at the center). Prior austenite grain boundaries in these specimens were revealed with a modified Winsteard's etchant (a mixture of 20 g picric acid, 100 ml ethyl alcohol, 2000 ml water, 50 ml sodium tridecylbenzene sulfonate, and a few drops of HCl as needed), while a 4 pct picral etchant containing one drop of HCl per 100 ml was used to reveal the general microstructure.

Thin foils for transmission electron microscopy (TEM) were prepared following standard procedures. Final electrochemical thinning was performed in a twin-jet apparatus with a solution of 10 pct perchloric acid/90 pct methanol at −50 °C. The foils were examined in a PHILIPS* EM430 electron microscope operating at 300 kV.

*PHILIPS is a trademark of Philips Instruments Corporation, Mahwah, NJ.

D. *Boron Autoradiography*

The distribution of boron in the present steels was revealed by an autoradiographic technique[13] in which samples were irradiated with thermal neutrons to activate boron atoms; these atoms subsequently underwent fission to produce tracks in a suitable solid detector film applied to the sample surface. Samples (about 1-mm-thick) for irradiation were removed from end-quenched plates, mounted in BAKELITE,* and polished accord-

*BAKELITE is a trademark of Union Carbide Corporation, Danbury, CT.

Table III. Results of End-Quench Hardenability Tests

ppm B/FRT/Delay*	Quench Temperature (°C)	Maximum Hardness (HRC)	50 Pct Martensite Location**	Cooling Rate† (°C/s)	Equivalent Jominy Position‡	D_I (mm)
0/980/13	946	21.7	—	—	—	20.3§
0/970/64	838	21.1	—	—	—	20.3§
0/980/100	802	23.1	—	—	—	20.3§
0/980/150	763	23.8	—	—	—	20.3§
0/870/24	835	25.6	—	—	—	20.3§
0/875/64	799	23.4	—	—	—	20.3§
0/870/104	763	22.6	—	—	—	20.3§
10/970/10	943	41.1	14.5	11.6	15.9	86.4
10/970/22	929	41.4	9.7	13.6	14.3	78.7
10/975/65	841	40.8	7.9	14.4	14.3	78.7
10/970/107	785	40.7	7.9	14.4	14.3	78.7
10/870/24	832	40.9	9.7	13.6	14.3	78.7
10/870/64	788	41.6	7.4	14.7	14.3	78.7
10/870/104	735	43.4	9.7	13.6	14.3	78.7
20/970/10	943	38.5	13.2	12.2	15.9	86.4
20/980/22	929	39.8	8.4	14.2	14.3	78.7
20/970/68	843	40.6	7.9	14.4	14.3	78.7
20/965/105	793	40.2	14.2	11.7	15.9	86.4
20/875/10	854	39.1	14.7	11.4	15.9	86.4
20/875/65	782	39.6	5.8	15.3	13.5	76.2
20/870/105	732	42.3	12.4	12.5	15.1	83.8
50/985/10	954	40.1	9.7	13.6	14.3	78.7
50/980/66	849	37.1	2.3	16.7	13.5	76.2
50/975/105	793	33.2	−10.9	21.1	11.9	71.1
50/870/24	832	34.6	− 4.6	19.2	12.7	73.7
50/870/64	779	30.9	−11.4	21.4	11.1	66.0
50/870/105	738	31.5	−15.5	22.8	11.1	66.0
100/980/10	957	35.3	− 2.8	18.6	12.7	73.7
100/980/65	849	33.5	− 6.9	20.0	11.9	71.1
100/980/105	799	37.1	− 2.8	16.4	13.5	76.2
100/980/118	782	24.4	—	—	—	<63.5
100/870/25	835	31.4	− 4.6	19.2	12.7	73.7
100/870/64	785	31.0	−36.8	28.3	10.3	63.5
100/870/104	738	31.6	−11.4	21.4	11.1	66.0

*Denotes nominal boron content, finish-rolling temperature (°C), and delay time prior to quenching (s).
**Location (millimeters above water surface) where hardness = 31 HRC.
†At the 50 pct martensite hardness location.
‡Millimeters from quenched end.
§Calculated on the basis of composition following Grossman and Bain.[12]

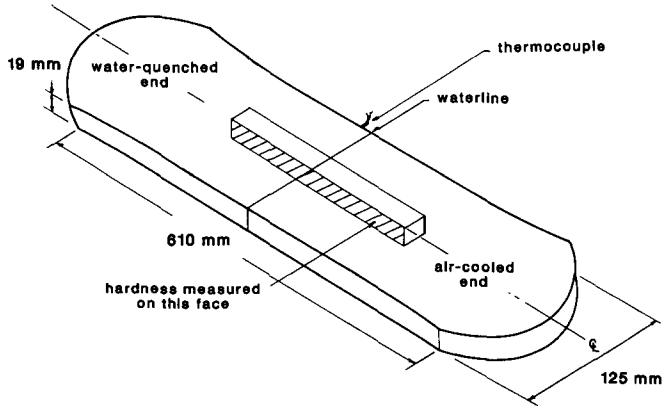

Fig. 4—Diagram of an end-quenched plate showing the location from which the hardenability specimen is removed.

ing to standard metallographic procedures. These samples were then coated with a cellulose nitrate detector film and irradiated to a fluence of 5×10^{14} neutrons/cm^2. The films were subsequently stripped from the samples and etched in an aqueous solution of 10 pct NaOH at 30 °C to 40 °C for 15 to 45 minutes. The films were also coated with a thin layer of gold to facilitate examination in an optical microscope with reflected light.

III. RESULTS

A. *Austenite Grain Structures*

Examples of the prior austenitic grain structures produced by the two deformation schedules used in this work are shown in Figure 7. For all steels, finishing at 980 °C

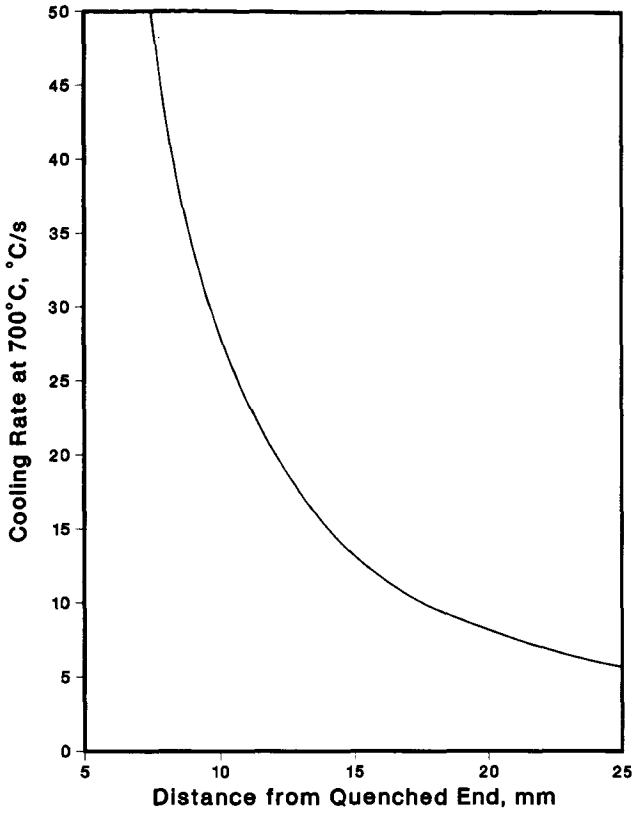

Fig. 5—Relationship between cooling rate and distance from the quenched end for a standard Jominy hardenability specimen.[10]

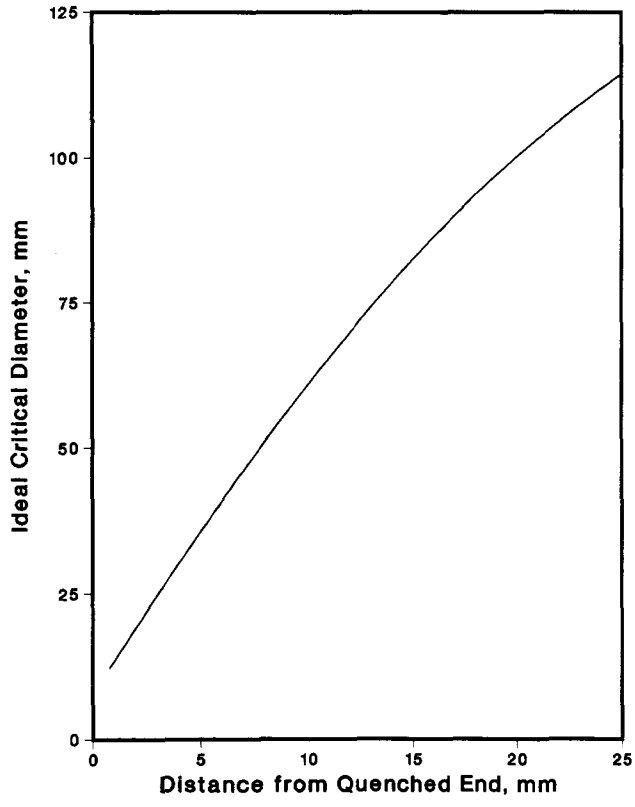

Fig. 6—Relationship between ideal diameter and the distance from the quenched end of a Jominy specimen at which a 50 pct martensitic microstructure is produced.[11]

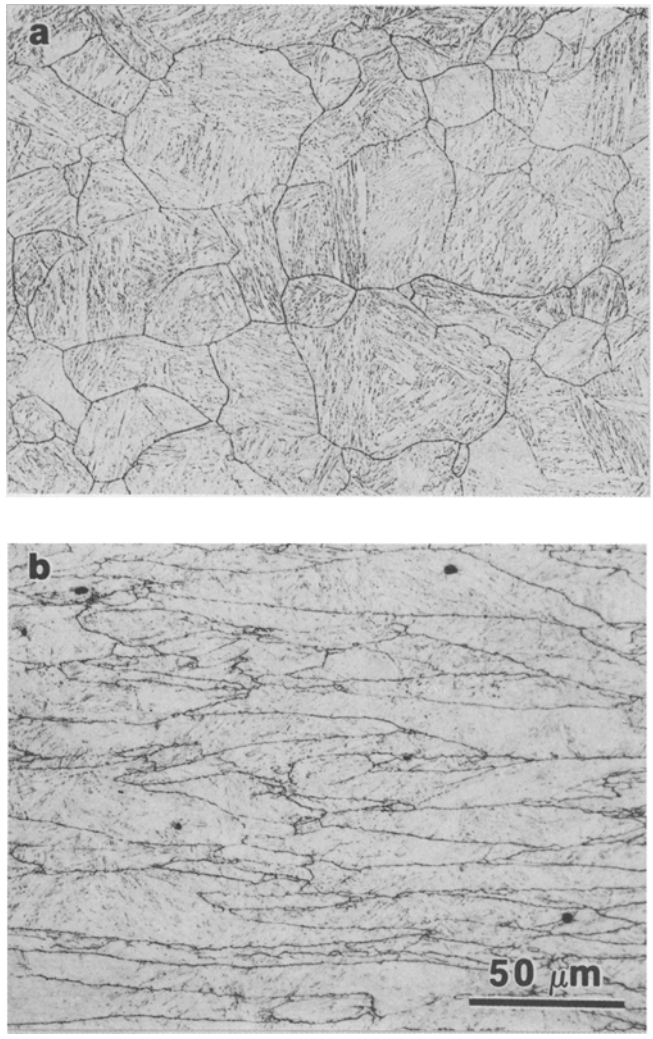

Fig. 7—Prior austenite grain structures after finishing at (*a*) 980 °C (20 ppm B steel) and (*b*) 870 °C (10 ppm B steel).

resulted in an essentially equiaxed austenitic grain structure (Figure 7(a)), whereas finishing at 870 °C resulted in severely deformed austenite grains (Figure 7(b)). Mean intercept grain sizes for both finishing temperatures are reported for each steel in Table IV, with the prior austenite grain "thickness" (the mean linear intercept length along a direction normal to the rolling plane) reported for the plates containing deformed prior austenite grains.

Table IV. Mean Intercept Prior Austenite Grain Sizes, μm*

Nominal B Content (ppm)	Finish-Rolling Temperature	
	980 °C	870 °C
0	27.9	11.8
10	38.4	12.1
20	28.1	10.0
50	31.4	15.0
100	32.6	28.9

*For plates finished at 870 °C, values represent intercept distance along a direction perpendicular to the rolling plane.

These results are for plates that were rolled with either a 60-second quenching delay (finishing temperature of 980 °C) or a 20-second quenching delay (finishing temperature of 870 °C). Although it is possible that grain growth occurred during the quenching delay for the plates rolled above the austenite recrystallization temperature, any grain size variation over the delay times used in this work is not expected to affect the hardenability results significantly. As indicated in Table IV, the grain sizes for plates finished at 980 °C were about 30 to 40 μm, and grain thicknesses for the plates finished at 870 °C were about 10 to 30 μm.

B. *Hardenability Tests*

Figure 8 shows the hardness variations along the end-quenched plates for a finish-rolling temperature of 980 °C and nominal quenching delays of 10, 60, and 100 seconds; Figure 9 shows similar data for the 870 °C finishing temperature. A line corresponding to the hardness of a microstructure consisting of 50 pct martensite (31 HRC for the present steels) is included in each plot. In any given test, the cooling rate required to achieve this hardness served as the basis for estimating the D_I (Section II–B) for the particular steel and processing conditions. Table III lists the hardenability parameters for each end-quenching test, including the hardness at the water-quenched end (the average of measurements obtained for locations 50 to 75 mm below the water surface), the location on each plate (and associated cooling rate) where the 50 pct martensite hardness was attained, the location on a standard Jominy bar with the same cooling rate, and the D_I corresponding to that cooling rate.

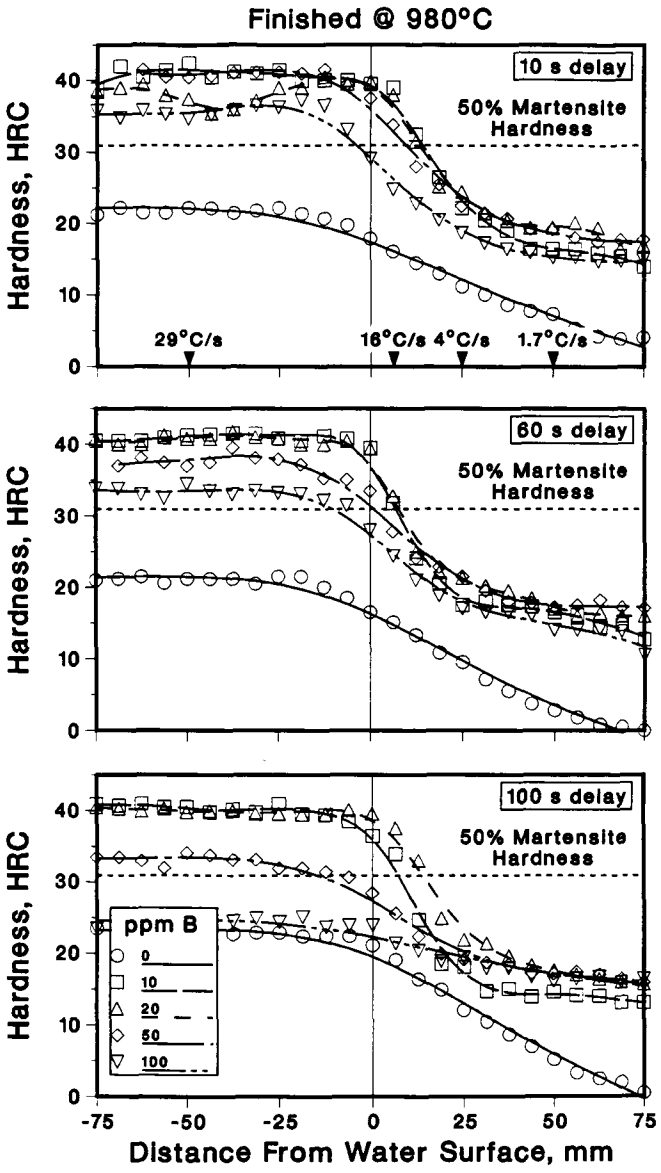

Fig. 8—Hardness *vs* distance from the water surface for end-quenched plates finished at 980 °C and air-cooled for 10, 60, and 100 s prior to quenching. Cooling rates at several positions are given in the upper plot.

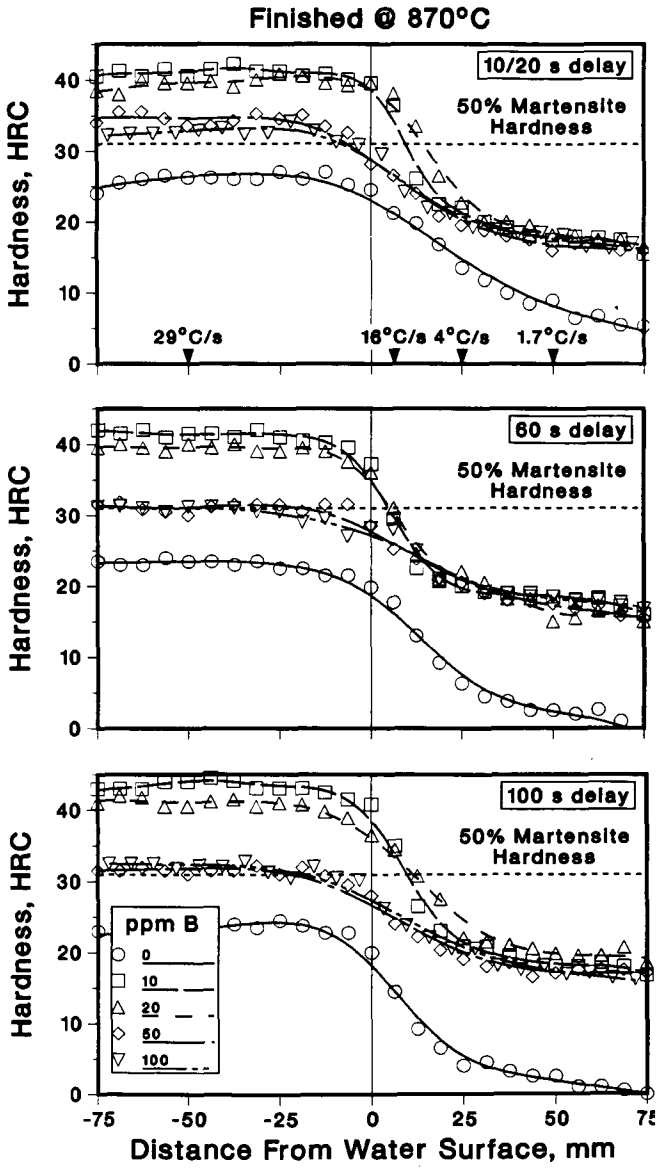

Fig. 9—Hardness *vs* distance from the water surface for end-quenched plates finished at 870 °C and air-cooled for 10 or 20, 60, and 100 s prior to quenching. Cooling rates at several positions are given in the upper plot.

1. *Effects of boron content on hardenability*

In general, the hardness values obtained for the B-treated steels ranged from a maximum of about 41 HRC at the water-quenched end of the plates to 10 to 20 HRC at the air-cooled end of the plates. (A hardness of 41 HRC is about what would be expected for an as-quenched, fully martensitic steel containing 0.2 pct C.) However, the hardness values obtained for the B-free steel were generally significantly lower than those for the B-treated steels, and this steel never exhibited a hardness higher than 26 HRC. This result was anticipated because the *calculated* D_I for this steel is only about 20 mm, whereas the *measured* D_I values for the B-treated steels generally varied between about 60 and 85 mm (Table III). The microstructures at the water-quenched end of the B-free plates consisted primarily of bainite with some islands of martensite (Figure 10). In contrast, the 10 and 20 ppm B steels generally were fully martensitic at the water-quenched end of each test plate (Figure 10), and the D_I values for these steels varied between 76 and 87 mm. Some bainite was generally present in the 50 and 100 ppm B steels, and the hardness profiles and D_I values for these steels were intermediate between the B-free steel and the 10 and 20 ppm B steels. Small, dark-etching features were also observed on metallographic specimens of the 50 and 100 ppm B steels (Figure 11), especially in specimens from plates which had been processed with quenching delays of 60 seconds and more. These features were distributed along prior austenite grain boundaries and, as shown below, were borocarbides that precipitated either during rolling or during the delay prior to quenching.

2. *Effects of processing parameters on hardenability*

For each of the steels containing 0, 10, and 20 ppm B, the end-quenching results for a given steel were generally very similar for both of the finishing temperatures

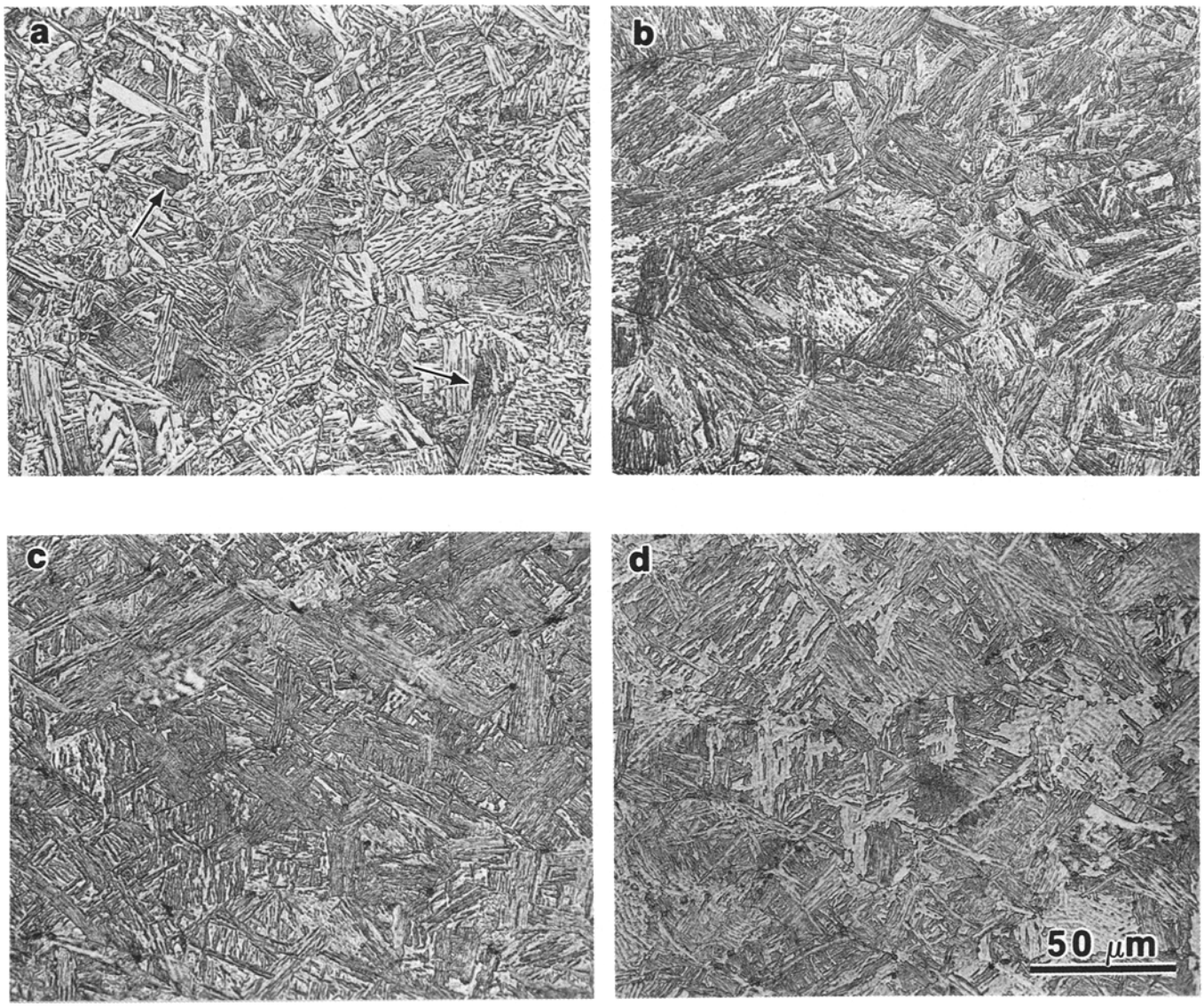

Fig. 10—Microstructures at the water-quenched end of hardenability specimens for a finish-rolling temperature of 980 °C and a quenching temperature of about 840 °C (60-s quenching delay): (*a*) 0 B, (*b*) 20 ppm B, (*c*) 50 ppm B, and (*d*) 100 ppm B. Arrows indicate martensite islands in the B-free steel.

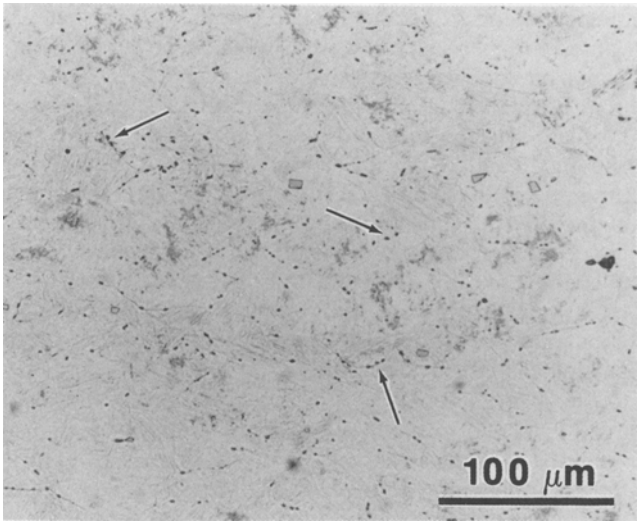

Fig. 11—Borocarbides (dark-etching features along prior austenite grain boundaries (arrows)) in the 50 ppm B steel after finishing at 980 °C and quenching at 849 °C (66-s quenching delay).

examined in this investigation. The measured D_I values (Table III) for the 10 and 20 ppm B steels also did not vary significantly with delay time; the variation of about 10 mm in the D_I values for these steels (76.2 to 86.4 mm) is probably near the limit of accuracy of the present end-quenching test.[8] In contrast, the transformation behavior of the 50 and 100 ppm B steels was much more sensitive to processing variables than were the lower B steels. The hardenability of these steels (in terms of both the maximum hardness and the D_I (Table III)) generally decreased with increasing delay time when these steels were finished at 980 °C. Decreasing the finishing temperature to 870 °C also generally resulted in lower hardenability compared with the 980 °C finishing temperature, and the transformation behavior was almost constant over the delay times examined here (the hardness profiles for 20-, 60-, and 100-second delays are very similar). As indicated above, dark-etching features that were probably borocarbides were detected along the prior austenite grain boundaries of these higher B steels in all cases except for when rolling was finished at 980 °C and the shortest quenching delay (10 seconds) was used.

C. *Boron Autoradiography*

The boron radiographs for the 10 and 20 ppm B steels indicated that segregation of B to the austenite grain boundaries had occurred in these steels under all conditions examined. Figures 12 and 13 show prior austenite grain boundaries in the 10 ppm B steel (after finishing at 980 °C) and the 20 ppm B steel (after finishing at 870 °C), respectively. In general, however, the austenitic grain structure was more difficult to resolve in the samples that were finished at 870 °C and contained deformed austenite grains. This may be a result of B segregation to deformation bands and subboundaries within the deformed grains, which presumably would reduce the overall contrast between the grain boundaries and the intragranular regions.

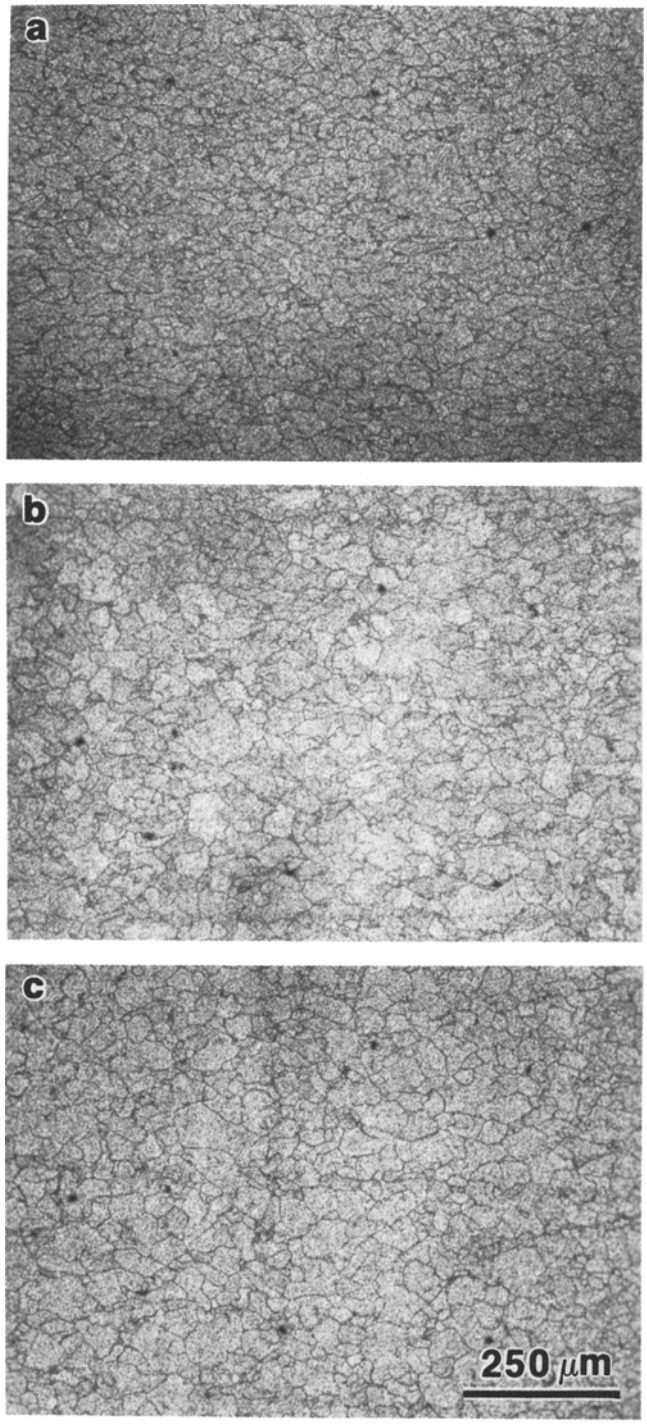

Fig. 12—Boron radiographs of the 10 ppm B steel after finishing a 980 °C and air cooling for (*a*) 7 s, (*b*) 65 s, and (*c*) 104 s prior t quenching.

After finishing at 980 °C with a short quenchin delay, the 50 ppm B steel showed segregation of B t the austenite grain boundaries (Figure 14(a)) similar t that observed for the 10 and 20 ppm B steel (Figure 12(a)). However, increasing the delay to 60 o 100 seconds (which, as mentioned above, significantl reduced the hardenability) resulted in the appearance o discrete grain boundary features (Figures 14(b) and (c))

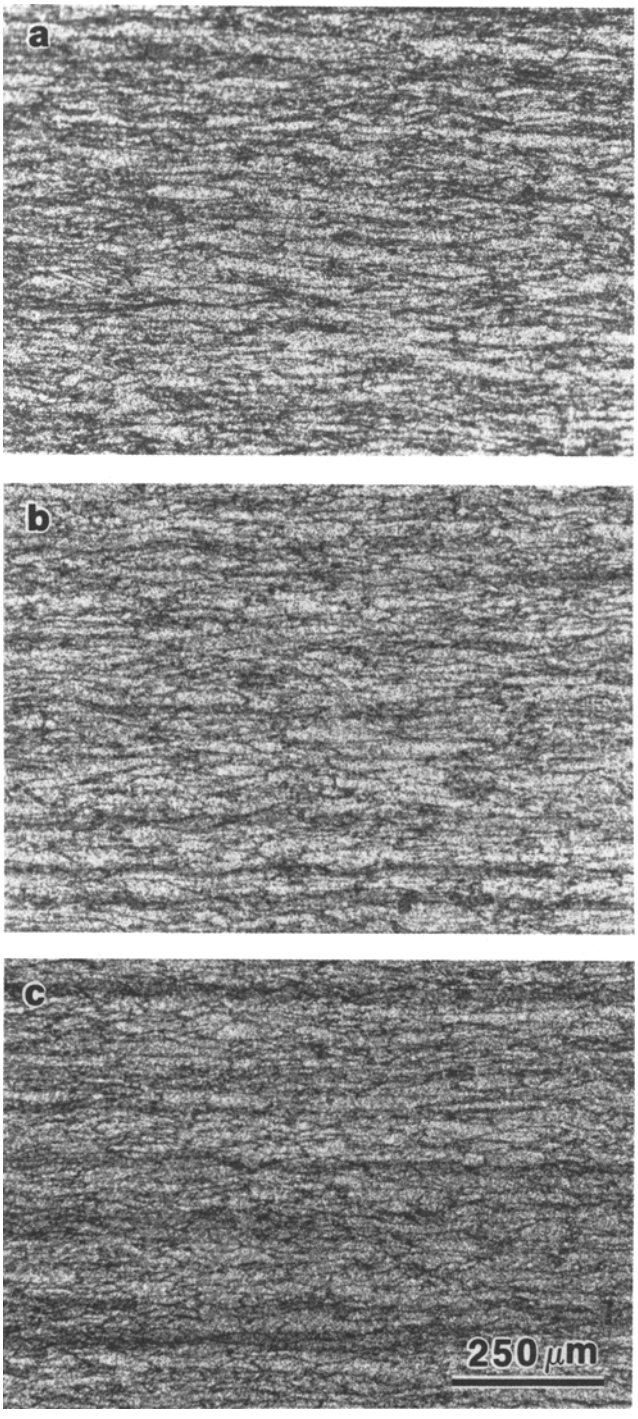

Fig. 13—Boron radiographs of the 20 ppm B steel after finishing at 870 °C and air cooling for (*a*) 10 s, (*b*) 65 s, and (*c*) 105 s prior to quenching.

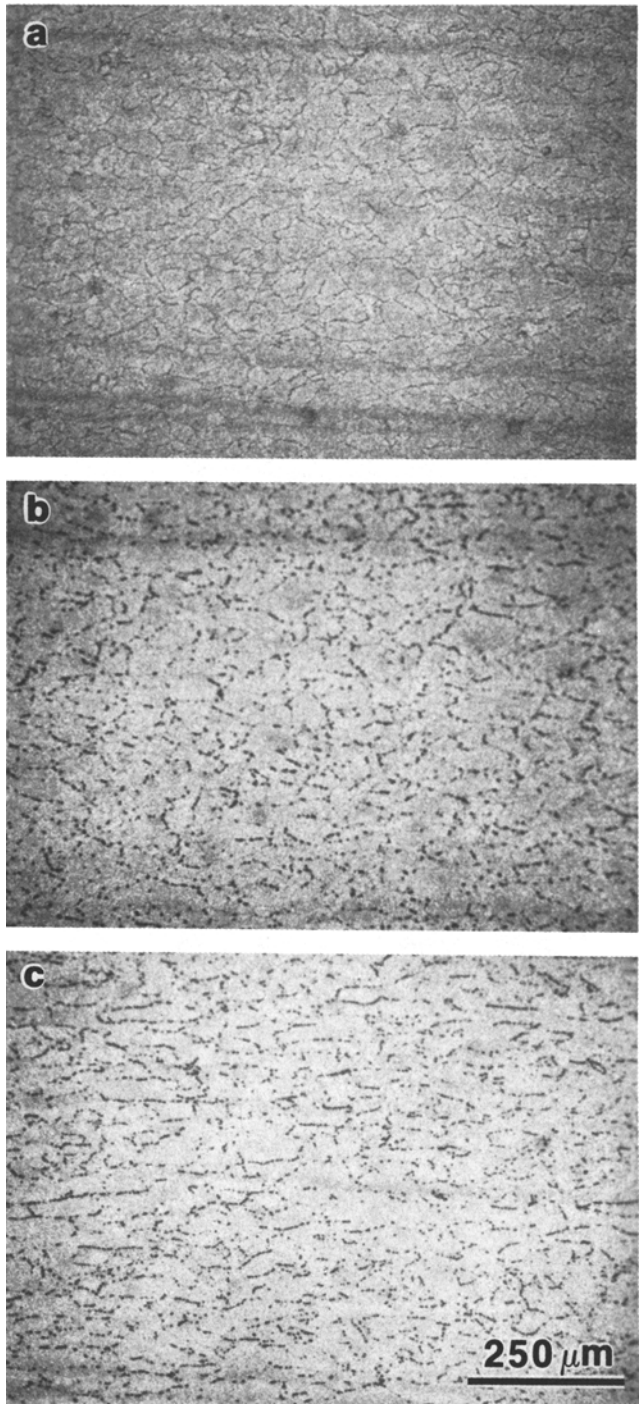

Fig. 14—Boron radiographs of the 50 ppm B steel after finishing at 980 °C and air cooling for (*a*) 10 s, (*b*) 66 s, and (*c*) 105 s prior to quenching.

and a continuous grain boundary network was no longer apparent. These grain boundary features appeared to be more numerous for the 100-second quenching delay than for the 60-second delay. Thin foils from the 100 ppm B steel finished at 870 °C and quenched with a 100-second delay were examined in the transmission electron microscope, and irregularly shaped precipitates about 0.1 to 1 μm in size were observed (Figure 15) along the prior austenite grain boundaries. Selected-area electron diffraction patterns from these precipitates were consistent with a face-centered cubic structure with a lattice constant of about 1.07 nm. Hence, these boron-containing particles are probably $M_{23}(C, B)_6$-type iron borocarbides which are cubic compounds with lattice constants of 1.06 to 1.07 nm[14] that have been reported to precipitate in B-treated steels with low soluble nitrogen contents.[15,16]

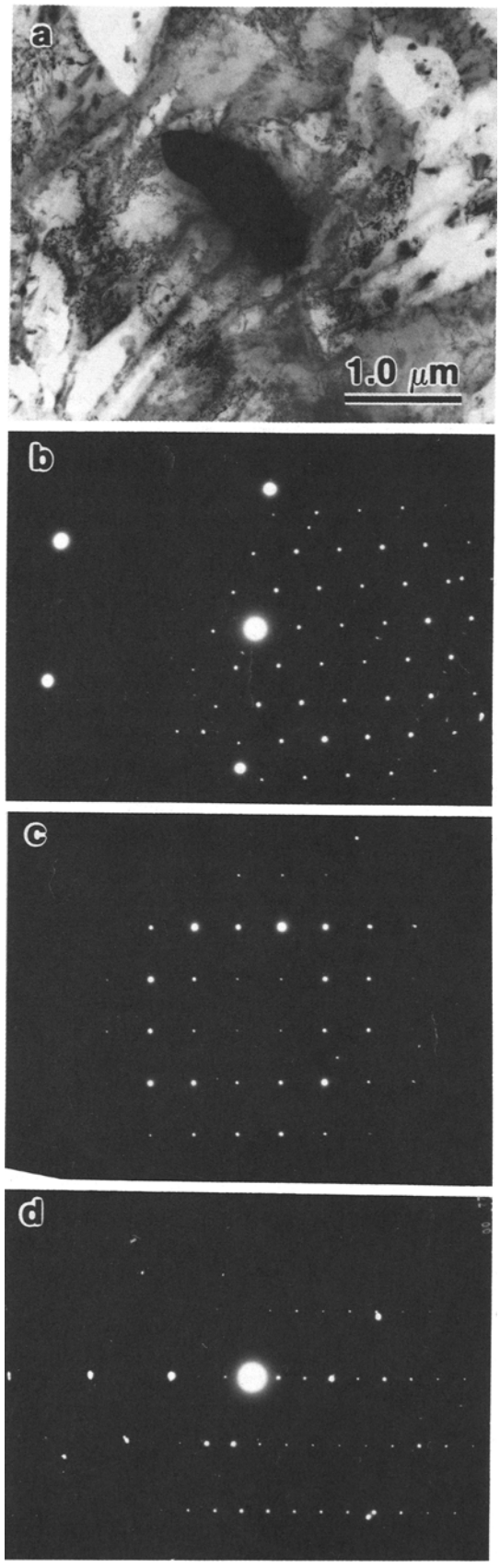

Fig. 15—An $M_{23}(C, B)_6$ particle (*a*) in the 100 ppm B steel after finishing at 870 °C and air cooling for 118 s prior to quenching. Selected-area [111], [223], and [123] electron diffraction patterns from this particle are shown in (*b*), (*c*), and (*d*), respectively.

IV. DISCUSSION

The present results show that the full boron hardenability increment was generally obtained in thermomechanically processed, direct-quenched steels containing 10 and 20 ppm B, even when quenching followed deformation of the austenite within times as short as 10 seconds. Therefore, it appears that a sufficient amount of boron diffuses to the austenite grain boundaries in these steels in a very short time. The distance over which boron atoms can diffuse during the quenching delay was calculated for each of the plates rolled during this study (as described in the Appendix). These calculations indicate that boron atoms can diffuse about 20 μm during a 10-second delay after finishing at 980 °C (or about 15 μm during a 10-second delay after finishing at 870 °C). This distance is comparable to the grain radius or half-thickness (the maximum diffusion distance); hence, even for this short delay, there should be adequate time for boron segregation to the austenite grain boundaries.* The longer delays allow for even more diffusion—a 100-second delay results in a diffusion distance of about 50 μm (or about 35 μm for a finishing temperature of 870 °C). In general then, for delay times of 10-seconds or more, there is sufficient time for boron atoms to diffuse to the austenite grain boundaries.

*Any additional nonequilibrium segregation of B during cooling by diffusion of boron atom–vacancy complexes[17] would accelerate the overall segregation kinetics.

The present results for samples that contained recrystallized austenite prior to direct quenching are generally consistent with the recent investigations of 0.1 wt pct C steels containing 10 ppm B,[3,4] in which the normal boron hardenability increment was obtained over a wide range of processing conditions, particularly when Ti (instead of Al) was used to getter free nitrogen.[3] However, Imanaka *et al.*[4] found that when static recrystallization occurred subsequent to deformation and the quenching delay was extremely short, there was inadequate time for the boron to diffuse to the newly created austenite grain boundaries. The steels evaluated in that study were reheated to 1150 °C and reduced in thickness from 50 to 30 mm in one pass at 900 °C. Delays of 3, 30, and 180 seconds prior to cooling (at 10 °C/s) were examined. The results showed that the full boron hardenability increment was not always obtained for the 3-second delay because static recrystallization and segregation of boron to the grain boundaries were not complete (for this 3-second delay, the effective boron diffusion distance would be only about 5 μm). However, in a commercial (plate mill) direct-quenching operation, a minimum quenching delay of 15 to 30 seconds would be anticipated (to allow for leveling of the plate and its transport to the quenching unit); hence, there should not be any operating limitations with regard to providing adequate time for sufficient grain boundary segregation of boron after finish-rolling.

While diffusion of boron to newly formed austenite grain boundaries is not expected to be a limiting factor in achieving maximum hardenability in steels containing recrystallized austenite, precipitation of

borocarbides prior to quenching is still of concern. Not only does precipitation remove elemental boron from the grain boundaries, but the precipitates themselves have been reported to act as ferrite nucleation sites.[15,16] Imanaka *et al.*[4] found that B-containing precipitates formed in samples that were held for 180 seconds prior to quenching. Their 10 ppm B steels were not Ti-treated to protect the B from N (although some of the Al present may have combined with some of the N); therefore, these precipitates were believed to be BN. No precipitation of any B-containing particles was detected in the present 10 and 20 ppm B steels, although a direct comparison between these two investigations is complicated by the differences in soluble nitrogen levels in the steels and in the quenching delays (which involved an isothermal hold in Reference 4). The precipitation of borocarbides in the present 50 and 100 ppm B steels, which had an adverse effect on hardenability, indicates that the boron level needs to be carefully controlled to obtain maximum hardenability in direct-quenched steels.

The present results also show that the decrease in the hardenability of the 50 and 100 ppm B steels with an increasing delay prior to quenching is more rapid for a finishing temperature of 870 °C than for a finishing temperature of 980 °C. This may be the result of *strain-induced* precipitation of borocarbides (along deformed austenite grain boundaries or deformation bands) for the lower finishing temperature. Presumably, the borocarbide precipitation kinetics would be more rapid in an unrecrystallized austenite compared to a recrystallized austenite. However, since the quenching temperatures for samples finished at 870 °C were generally lower than those for the 980 °C finishing temperature, a higher borocarbide supersaturation may also contribute to the more rapid precipitation kinetics at a lower finishing temperature.

The behavior of boron in the present steels is summarized in Figure 16 which plots quenching temperature *vs* the product of the boron and carbon contents of each of the steels (proportional to the borocarbide supersaturation at a given temperature). Solid symbols in Figure 16 represent conditions under which borocarbide precipitates were detected after quenching, while half-filled symbols represent conditions under which boron was segregated to the austenite grain boundaries and no precipitates were detected. This figure also includes data from previous investigations,[16,18,19] in which the behavior of boron was investigated in austenitized-and-quenched steels similar in carbon content to those of this study. (The steels used in these prior studies also contained Ti additions to stabilize N.) Although there are considerable differences in the time/temperature treatments employed in these investigations, the data define an approximate boundary (continuous curve in Figure 16) which can be used to predict whether boron will be segregated or precipitated for a given steel composition and quenching temperature. Raghavan and Ghosh[20] conclude that $M_{23}(C, B)_6$ is not stable above 965 °C; hence, a dashed line at 965 °C is included in Figure 16 to represent the maximum temperature at which borocarbide precipitation could be expected. Consistent with this, Keown and Pickering[18] and He *et al.*[19] found no evidence of precipitation or segregation in steels containing

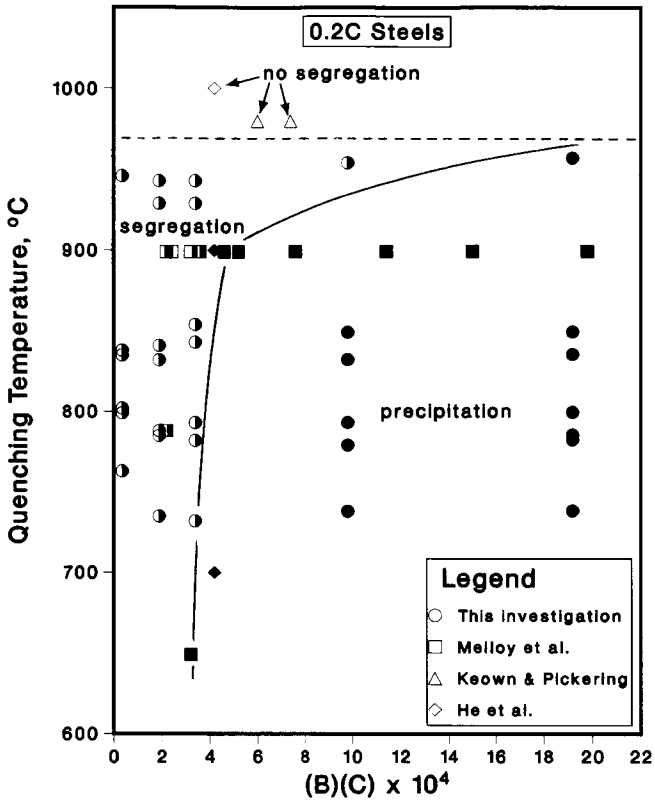

Fig. 16—State of the boron (segregated to austenite grain boundaries or precipitated at austenite grain boundaries) for the various combinations of quenching temperature and "solubility product" ((B)(C)) examined. Data from Refs. 16, 18, and 19 are also included, as well as a line representing the maximum temperature at which $M_{23}(C, B)_6$ borocarbides are stable.[20]

35 to 42 ppm B after quenching from 980 °C and 1000 °C, respectively (open symbols in Figure 16).

To summarize, the current results indicate that a boron content in the range of 10 to 20 ppm should provide a hardenability increment in thermomechanically processed, direct-quenched steels similar to that obtained for conventionally quenched-and-tempered steels. When the boron level is within this range, this boron hardenability increment should be obtainable over a wide range of processing conditions. Specifically, we have found the hardenability of steels containing 10 and 20 ppm boron to be relatively constant for finish-rolling temperatures of 980 °C and 870 °C and for quenching delay times between 10 and 100 seconds. This range of delay times should cover the range that would be encountered in a commercial in-line plate mill quenching unit. In contrast, steels containing 50 and 100 ppm boron were susceptible to the precipitation of borocarbides prior to quenching, with a resultant decrease in hardenability.

V. CONCLUSIONS

The results reported here support the following conclusions regarding the effects of boron content, deformation temperature, and delay time prior to quenching on the hardenability of thermomechanically processed, direct-quenched steels.

1. As is the case for conventionally quenched-and-tempered steels, a boron content of 10 to 20 ppm appears to provide a full hardenability increment from this element in thermomechanically processed, direct-quenched steels.
2. Borocarbide precipitation occurs in steels containing 50 ppm or more B (especially when the quenching temperature is low as a result of rolling at low temperatures or a long delay prior to quenching) and results in lower hardenability compared to steels containing 10 and 20 ppm B.
3. The hardenability of steels containing 10 and 20 ppm B was insensitive to the delay prior to direct quenching over the range of times examined here (10 to 100 seconds).

APPENDIX

Calculation of effective boron diffusion distance

This appendix describes how the diffusion distance calculations were performed. The distance, δ, over which an atom can diffuse during a given time, t, at a given temperature is given by

$$\delta = (Dt)^{1/2} \quad [A1]$$

where D is the diffusion coefficient. Diffusion coefficients are usually expressed in the form

$$D = D_0 \exp(-Q/RT) \quad [A2]$$

where D_0 is a constant, Q is the activation energy for diffusion, R is the gas constant, and T is the absolute temperature. The diffusion coefficient for boron in austenite, $D(B, \gamma)$, has been reported as[21]

$$D(B, \gamma) = 2 \times 10^{-4} \exp(-87{,}864/RT) \quad m^2/s \quad [A3]$$

where R is 8.314 J/mole·K. The effective diffusion distance for boron in austenite is then

$$\delta = [2 \times 10^{-4} \exp(-87{,}864/RT) \cdot t]^{1/2} \quad [A4]$$

For an isothermal treatment, the calculation of the effective diffusion distance is straightforward—one simply substitutes the temperature and time into Eq. [A4]. The situation is more complex under conditions of continuous cooling, such as for plates which are air-cooled prior to quenching. In cases where the temperature is not constant, δ can be expressed as

$$\delta = [\int D(t)\, dt]^{1/2} \quad [A5]$$

where $D(t)$ is the diffusion coefficient (which is now time-dependent), and dt is the differential of time. Equation [A5] can be converted to an expression with only a temperature variable by making the following substitution

$$dt = \frac{dT}{dT/dt} \quad [A6]$$

If a constant cooling rate (dT/dt) is assumed, then Eq. [A5] can be rewritten as

$$\delta = [2 \times 10^{-4} k \int \exp(-87{,}864/RT)\, dT]^{1/2} \quad [A7]$$

where k is the reciprocal of the cooling rate. Equation [A7] is evaluated with the finish-rolling and quenching temperatures as the limits of integration. For each experiment in this study, these temperatures, as well as the average cooling rate, were obtained directly from a strip chart recording.

ACKNOWLEDGMENTS

The authors gratefully acknowledge the assistance with the experimental work provided by R.J. August, J.W. Burkit, K.E. Downey, J.C. Hlubik, N. Katynski, J.R. Kilpatrick, R.R. Lichty, and C. Santos, Jr. We also thank Dr. D.C. Rorer and the Brookhaven National Laboratory, Upton, NY, for performing the neutron irradiations.

REFERENCES

1. D.T. Llewellyn and W.T. Cook: *Met. Technol.*, 1974, vol. 1, pp. 517-29.
2. *Boron in Steel*, S.K. Banerji and J.E. Morral, eds., TMS-AIME, Warrendale, PA, 1980.
3. N. Shikanai, M. Kurihara, and H. Tagawa: *Proc. Int. Conf. on Physical Metallurgy of Thermomechanical Processing of Steels and Other Metals* (THERMEC-88), The Iron and Steel Institute of Japan, Tokyo, 1988, pp. 98-105.
4. M. Imanaka, H. Terasima, C. Siga, S. Ueda, and T. Tanaka: *J. Iron Steel Inst. Jpn.*, 1988, vol. 74, pp. 167-74.
5. K.A. Taylor and S.S. Hansen: *Proc. Int. Symp. on Accelerated Cooling of Rolled Steel*, G.E. Ruddle and A.F. Crawley, eds., Pergamon Press, Elmsford, NY, 1988, pp. 85-101.
6. Y. Tomita: *Mater. Sci. Technol.*, 1988, vol. 4, pp. 613-20.
7. D. Dulieu, D.J. Latham, J.W. Bannister, and S. Gibson: *Iron Steel*, 1972, vol. 45, pp. 277-84.
8. K.A. Taylor and S.S. Hansen: *Proc. 6th Int. Congr. on Heat Treatment of Materials*, ASM INTERNATIONAL, Metals Park, OH, 1988, pp. 137-42.
9. B.M. Kapadia, R.M. Brown, and W.J. Murphy: *Trans. AIME*, 1968, vol. 242, pp. 1689-94.
10. W.E. Jominy: in *Hardenability of Alloy Steels*, ASM, Cleveland, OH, 1939, pp. 66-94.
11. C.T. Kunze and J.E. Russell: in *Hardenability Concepts with Applications to Steel*, D.V. Doane and J.S. Kirkaldy, eds., TMS-AIME, Warrendale, PA, 1978, pp. 290-308.
12. M.A. Grossman and E.C. Bain: *Principles of Heat Treatment*, ASM, Metals Park, OH, 1964, pp. 75-127.
13. T.B. Cameron and J.E. Morral: in *Boron in Steel*, S.K. Banerji and J.E. Morral, eds., TMS-AIME, Warrendale, PA, 1980, pp. 61-79.
14. P. Rogl, J.C. Schuster, and H. Nowotny: in *Boron in Steel*, S.K. Banerji and J.E. Morral, eds., TMS-AIME, Warrendale, PA, 1980, pp. 33-43.
15. Y. Ohmori: *Trans. Iron Steel Inst. Jpn.*, 1971, vol. 11, pp. 339-48.
16. G.F. Melloy, P.R. Slimmon, and P.P. Podgursky: *Metall. Trans.*, 1973, vol. 4, pp. 2279-89.
17. R.G. Faulkner: *J. Mater. Sci.*, 1981, vol. 16, pp. 373-83.
18. S.R. Keown and F.B. Pickering: *Met. Sci.*, 1977, vol. 11, pp. 225-34.
19. X.L. He, Y.Y. Chu, and J.J. Jonas: *Acta Metall.*, 1989, vol. 37, pp. 2905-16.
20. V. Raghavan and G. Ghosh: *J. Alloy Phase Diagrams*, 1986, vol. 2, pp. 77-92.
21. P.E. Busby, M.F. Warga, and C. Wells: *J. Met.*, 1953, vol. 5, pp. 1463-68.